Ferroelectric and antiferroelectric liquid crystals for optical phase modulation

Leonid Beresnev[1], Thomas Weyrauch[1], Wolfgang Dultz[2], and Sergei Pikin[3]

[1]U.S. Army Research Laboratory, 2800 Powder Mill Road, Adelphi, MD 20783, USA
[2]Deutsche Telekom AG, Am Kavalleriesand 3, 64276 Darmstadt, Germany
[3]Institute of Crystallography, Russian Academy of Sciences, Leninskii prospect 59, 117333 Moscow, Russia.

ABSTRACT

A novel liquid crystalline material for optical phase modulation is proposed. The material consists of banana shaped dimer molecules, which form a lamellar phase, e. g. a smectic phase. A helical superstructure is induced by means of chiral fragments included in the molecular structure. Due to polyphilic segregation of hydrogenated and fluorinated molecule segments a cancellation of transversal dipole moments can be avoided and a net polarization of single layers will be obtained. The polarized layers may form ferroelectric or antiferroelectric structures. Application of an electric field in light propagation direction will deform the helix until total unwinding without reorienting the optical axes of the material, but changing the refractive index for one polarization direction. An estimation of the refractive indices of the material, its index modulation capability and the behavior under electric field is presented in this paper. The possible application of the material in phase modulators is discussed.

Keywords: Optical phase modulation, banana shaped liquid crystals, deformed helix ferroelectric effect

1. INTRODUCTION.

Materials with an variable refractive index are considered among the most basic electrooptical media for control of light beam properties. The change of the phase of light waves is the fundamental tool for the design of many adaptive optics systems [1], e. g. astronomical [2] and ground to ground imaging devices [3], optical communication systems, laser lidars, systems for optical turbulence simulation [4], etc. Such materials have potential for fast, high resolution and low costs wavefront control. Often used photorefractive materials have a too slow time response, a small change of refractive index and a small aperture size. Solid electrooptical crystals, e. g. $LiNbO_3$, have a very small change of the refractive index per unit length of the optical path, small aperture and high driving voltage.

Liquid crystals (LCs) as media with electrically controlled optical parameters, e. g. deviation and deformation of the local refractive index indicatrix have been considered as perspective materials for wavefront control during the last decade. The main electrooptical effects in liquid crystals are accompanied by a simultaneous change of both, phase and polarization. The latter is an undesirable effect for adaptive optics systems and other applications where phase-only modulation is required. Only the S-effect in nematic liquid crystals can provide so far a pure phase change of linearly polarized light with the polarization plane along the director of the parallel aligned nematic liquid crystal. This is widely used in pixelized electrically controlled phase modulators [5] as well as in optically addressed spatial light modulators (SLM) in connection with a photoconducting layer [6].

In both cases the operation speed of SLMs is restricted to several tens of milliseconds for a phase modulation depth of the order of 2π. To obtain a significant phase change $\Phi > 2\pi$ at the usual refractive index anisotropy $\Delta n \sim 0.2$, the LC cell thickness d should be of the order of 5 µm for red light. Because the relaxation time of nematic liquid crystal depends strongly on the cell thickness [7], it will be not less than tens of milliseconds in that case. Consequently the resulting operation rate for commonly used nematic LC based wavefront correctors can not exceed several Hz, though in some special electronic schemes a faster operation even until hundred Hz with a small change of the wavefront is possible [8].

High-Resolution Wavefront Control: Methods, Devices, and Applications II,
John D. Gonglewski, Mikhail A. Vorontsov, Mark T. Gruneisen, Editors,
Proceedings of SPIE Vol. 4124 (2000) © 2000 SPIE. · 0277-786X/00/$15.00

2. CONVENTIONAL DEFORMED HELIX FERROELECTRIC (DHF) LIQUID CRYSTALS

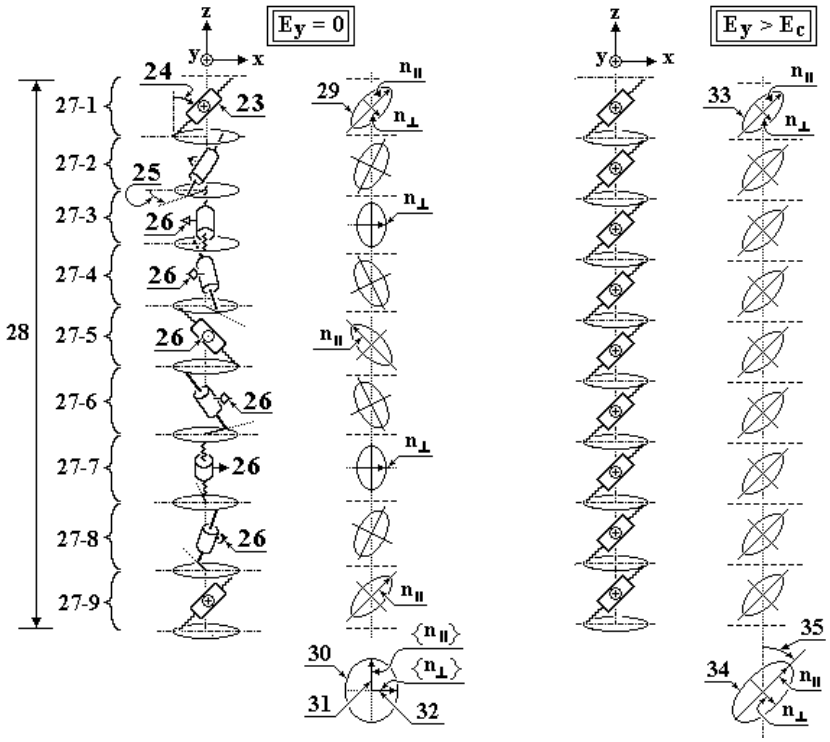

Figure 1. *Strongly twisted chiral smectic C liquid crystal and the change of the refractive index indicatrix (30) under an electric field E_y. The deviation of the refractive index ellipsoid on angle (35) takes place together with the deformation of the ellipsoid. One turn of helix (28) is shown.*

Chiral smectic ferroelectric liquid crystals (FLCs) [9] have much faster operation rate compared to nematic liquid crystals and the response time can be in the microsecond range [10]. The main electrooptical property of FLCs considered so far for applications is the electrically controlled switching [11], or the deviation of the optical indicatrix in the plane of transparent electrodes [12]. The change of refractive indices is considered as very small and the change of phase is negligible in FLC cells with commonly used thickness 1 - 1.5 µm. A higher change of refractive index was found in ferroelectric liquid crystals with a strongly twisted helical structure (Fig. 1) with the pitch of helix shorter than the wavelength.

The so-called DHF (deformed helix ferroelectric) effect [12, 13] is characterized in that an electric field E_y applied along the smectic layers 27-1, 27-2,..., 27-9... (cf. Fig. 1) induces a significant deformation of the refractive index indicatrix 30 at comparable small values of the applied voltage in the range of units of Volts. This deformation is related to the change of the uniform distribution of the azimuthal tilt 25 of the inclination plane up to the state, where the inclination planes of all smectic layers 27-1...27-9... have the same orientation perpendicular to the electric field E_y. The averaged refractive index ellipsoid 30 is deformed into the refractive index ellipsoid 34 which is equal to the molecular one (i. e. 33). This deformation takes place due to interaction of the electric field E_y applied to the smectic layers along the direction y with the dipole moments 26 of the molecules. The response time can be of the order of hundreds of microseconds [12, 13, 14] and doesn't depend on driving voltage. The change of the anisotropy of the refractive index between the electric field free state $\{\Delta n\} = \{n_{\|}\} - \{n_{\perp}\}$ and the unwound uniform state $\Delta n = n_{\|} - n_{\perp}$ can be of the order of 0.05. Here $\{n_{\|}\}$ and $\{n_{\perp}\}$ are the components 31 and 32 along the layer normal and along the layers of the averaged refractive index ellipsoid 30, respectively. $n_{\|}$ and $n_{\perp}$ are the refractive indices along and perpendicular to the molecular axes, respectively. The change of the refractive index of DHF materials under an applied electric field was tested in devices as electrically controlled Fabri-Perot etalons [15] and phase gratings applied for fast adaptive lenses [16]. In case of a change of the refractive index $\delta(\Delta n) = \Delta n - \{\Delta n\} = 0.05$, relatively thin cells are needed (thickness $d \approx$ 10-12 µm) to obtain a phase shift 2π. Due to the independence of the electrooptical response time from the cell thickness there is the possibility to design SLMs with gray scale phase modulation at low driving voltages of the order of 5 V and a fast response time in the range of 100 µs, that is 2-3 orders of magnitude faster than the operation speed of nematic liquid crystals.

The main drawback of this conventional DHF materials is the strong change of the polarization of the transmitted light beam, which leads to an unacceptable level of light wave disturbance apart from phase modulation. This disadvantage is connected with the inherent simultaneous change of all parameters of the refractive index ellipsoid 30 under influence of an electric field: The change of the excentricity of the ellipsoid $e = \{\Delta n\}/\Delta n$ is accompanied with an angular deviation of the orientation of the long axis $\{n_{\|}\}$ of the ellipsoid approximately proportional to the electric field [13, 14].

3. BANANA SHAPED DHF MATERIALS

1. Basic Approach

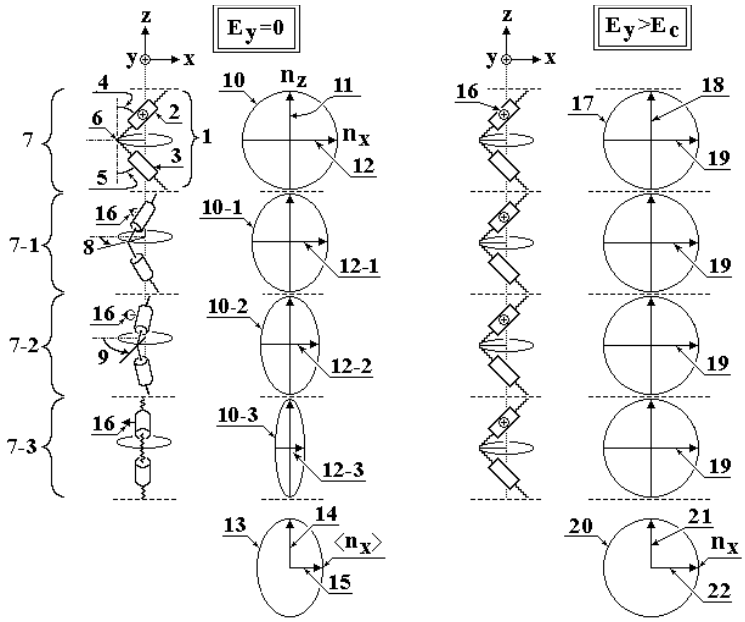

Figure 2. *The banana shaped structure of the proposed molecules 1 composing the smectic liquid crystal for phase modulation. The averaged refractive index ellipsoid 13 conserves its orientation along the normal z to the smectic layers 7, 7-1, 7-2 … in the helical structure. Under the action of an electric field E_y applied along the smectic layers the refractive index $<n_x>$ perpendicular to the normal z does change. A quarter part of an total turn of the helix is shown.*

In this paper ferroelectric and antiferroelectric liquid crystalline materials are proposed, which allow for phase modulation only (cf. Fig. 2). The molecules 1 of the proposed liquid crystal consist of two central electronically polarizable cores 2 and 3 connected with hydrocarbon, siloxane and/or perfluorinated chaines. These cores form a chevron or banana shaped dimer molecule. The cores 2 and 3 form the angles 4 and 5 of opposite signs with the normal to the smectic layers . The tips 6 of the chevron or banana like molecules precess with a uniform change of the azimuth angle 8, 9, if one goes along the normal *z* to the smectic layers. One turn of precession corresponds to one pitch of helix, which should be less than light wavelength. Molecules form a layer structure, for instance a smectic phase with the layers 7, 7-1, 7-2, 7-3 etc. For any change of the azimuths of the tips 6 of the dimer molecules the averaged refractive index ellipsoid 13 can be calculated by averaging of ellipsoids 10, 10-1, 10-2, 10-3....over the distance *z* of one pitch. The long axes 11 of these ellipsoids are always directed along *z*. Application of an electric field to the proposed material induces a change of the averaged refractive index ellipsoid 13 in such a manner that the long axis 14 conserves its value and orientation, whereas the perpendicular component 15 of the averaged refractive index 13 increases up to the value 22.

Even at a weak electric field E_y the chevron planes as well as all tips 6 have the tendency to be oriented in a plane perpendicular to the electric field. In a cross-section of the averaged refractive index ellipsoid the axis 15 along the smectic layer *x* and perpendicular to the electric field E_y will be increased, whereas the axis 14 along the normal *z* to the smectic layers will be unchanged. The component of the ellipsoid along the electric field and along the smectic layer decreases at such deformation.

The helical structure of the discussed smectic material is induced by a chiral fragment in one or both external tails of the molecules. These fragments induce also the spontaneous polarization with the local dipole moments 16 of the molecules along the smectic layers and perpendicular to the molecular chevron plane. Due to interaction of these molecular dipole moments 16 a weak electric field E_y is able to deform the helical structure up to total unwinding of the helix (right part of Fig. 2). The averaged refractive index ellipsoid 13 transforms to the molecular ellipsoid 20 without a change of the index 14 or 21 along the normal *z* to the smectic layers.

The component 22 of the refractive index ellipsoid 20 transforms from the averaged component 15 to the molecular one (i. e. 22) with a smooth increase under an increasing electric field E_y. It means that for light polarized along the smectic layer *x* a phase shift will takes place without any deviation of the polarization plane. The value of the phase change $\delta\Phi$ is determined by the difference between the indicatrix components 22 and 15, that is $\delta n_x = \langle n_x \rangle - n_x$, and $\delta\Phi = d\,(\langle n_x \rangle - n_x)$, where *d* is the cell thickness.

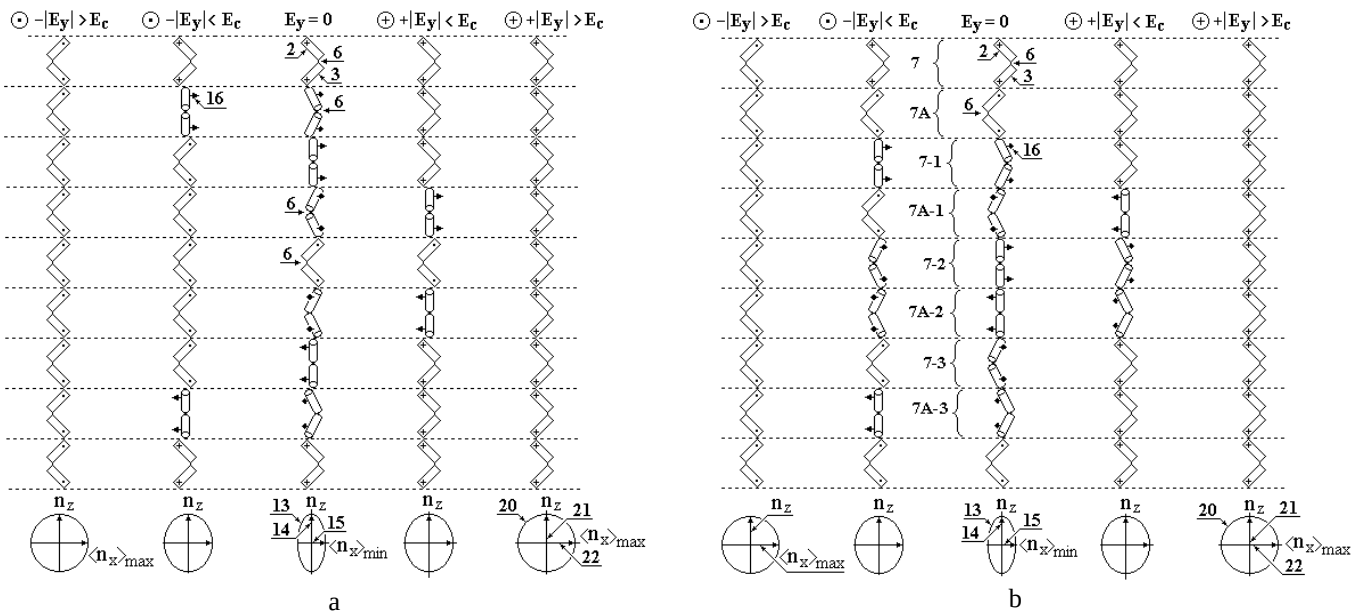

Figure 3. *Ferroelectric (a) and antiferroelectric (b) packing of the chiral banana shaped molecules. Tips 6 of dimer molecules in neighbor layers are directed in the same or opposite direction for ferroelectric or antiferroelectric materials, respectively. The gray scale for the change of the component* $<n_x>$ *of the averaged refractive index 13 under electric field* E_y *from* $<n_x>_{min}$ *to* $<n_x>_{max}$ *is indicated. A full turn and a half turn for the non-deformed helix are shown for the ferroelectric and antiferroelectric material, respectively.*

The directions of the chevron edges (tips 6) in neighbor smectic layers may have the same (Fig. 3a) or opposite (Fig. 3b) orientations. The ferroelectric or antiferroelectric molecular packing, respectively, will determine in these cases the interaction of the sum dipole moments of the smectic layers with the external electric field applied along the smectic layers. In both cases the limit states corresponding to high electric voltages, are optically similar to each other (see Figures 3a,b - left and right columns), only the directions of tips 6 are opposite. For small voltages, less than the threshold voltage of untwisting E_c, a gray scale variation of the refractive index component $<n_x>$ from the value $<n_x>_{min}$ to $<n_x>_{max}$ (Fig. 3) takes place when the voltage is increased from 0 to $E_y = E_c$.

2. Calculation of the possible phase modulation

For the calculation of the refractive indices of the helical structure of banana shaped molecules we assume two equal refractive index ellipsoids 2' and 3' (with identical values but opposite sign of inclinations 4 and 5 of their long axes $n_{\|}$) of the constituent parts 2 and 3, respectively. We consider for simplicity that the planes of molecules are perpendicular to smectic layers, though for known banana shaped smectic phases a significant deviation of molecular planes from the normal to the smectic surfaces was found [22]. If the helix pitch is smaller than the wavelength, light propagation is determined by the average optical properties rather than by the locally varying orientations of optical axes. Thus, effective refractive indices are calculated by averaging the local tensor of the dielectric susceptibility at optical frequencies over a full pitch of the helix (i. e. over a full turn of the azimuth angle φ), considering all possible orientations of the indicatrix ellipsoids of the sub-structures. In a first step the refractive indices of the dimer molecules are calculated as the average of the properties of the two sub-units 2 and 3 (cf. Fig. 4). The dielectric properties of the sub-unit 2 may be described by the tensor

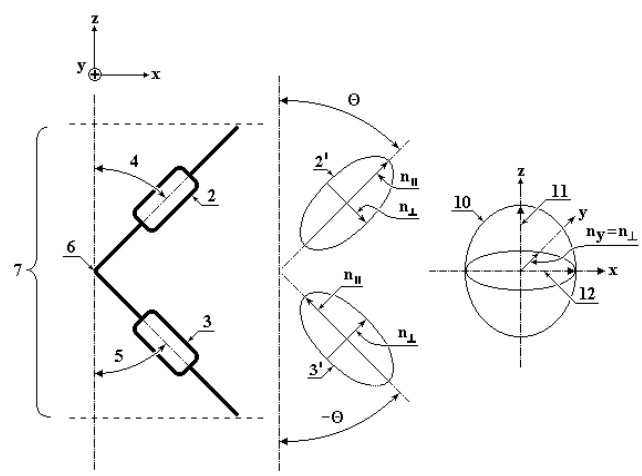

Figure 4. *The optical refractive indices 2' and 3' of the constituent parts 2 and 3 of the banana shaped dimer molecules, and the effective refractive index ellipsoid 10, describing the optical properties of the whole dimer molecule.*

$$\varepsilon^{mol} = \begin{bmatrix} \varepsilon_\perp & 0 & 0 \\ 0 & \varepsilon_\perp & 0 \\ 0 & 0 & \varepsilon_\parallel \end{bmatrix} = \begin{bmatrix} n_\perp^2 & 0 & 0 \\ 0 & n_\perp^2 & 0 \\ 0 & 0 & n_\parallel^2 \end{bmatrix}, \tag{1}$$

when the molecular long axis is chosen to be parallel to the *z*-axis. For the helical structure however, it is appropriate to choose the *z*-axis to be parallel to the helical axis and one must consider the tilt of the sub-units. If we assume that the molecule is oriented within the *xz*-plane (cf. Fig. 5), the dielectric tensor of sub-unit 2 is obtained considering a rotation around the *y*-axis by the tilt angle θ, which gives

$$\varepsilon(2) = \begin{bmatrix} \varepsilon_\perp \cos^2\theta + \varepsilon_\parallel \sin^2\theta & 0 & -\Delta\varepsilon \sin\theta\cos\theta \\ 0 & \varepsilon_\perp & 0 \\ -\Delta\varepsilon \sin\theta\cos\theta & 0 & \varepsilon_\perp \sin^2\theta + \varepsilon_\parallel \cos^2\theta \end{bmatrix}, \tag{2}$$

where $\Delta\varepsilon = \varepsilon_\parallel - \varepsilon_\perp$. The tensor ε(3) for the sub-unit 3 is obtained by a similar rotation by the angle π-θ. ε(3) is different from ε(2) only in respect to an inverse sign of the components ε_{xz} and ε_{zx}. The tensor ε(1) of the whole banana shaped dimer molecule is the average of the tensors ε(2) and ε(3) and is given by:

$$\varepsilon(1) = \begin{bmatrix} \varepsilon_\perp \cos^2\theta + \varepsilon_\parallel \sin^2\theta & 0 & 0 \\ 0 & \varepsilon_\perp & 0 \\ 0 & 0 & \varepsilon_\perp \sin^2\theta + \varepsilon_\parallel \cos^2\theta \end{bmatrix} \tag{3}$$

Because of the particularly chosen geometry (the molecules are oriented within the *xz*-plane), this tensor describes also the state, when the helical structure is totally unwound by an electric field above the threshold and directed along the *y*-axis (cf. right side of Fig. 2). We can thus easily extract the refractive indices of this structure from equation 3:

$$n_x = \sqrt{n_\perp^2 \cos^2\theta + n_\parallel^2 \sin^2\theta} \tag{4a}$$

$$n_y = n_\perp \tag{4b}$$

$$n_z = \sqrt{n_\perp^2 \sin^2\theta + n_\parallel^2 \cos^2\theta} \tag{4c}$$

As an example the effective refractive indices n_x, n_y and n_z of the untwisted state in dependence on the tilt angle θ, calculated according to equations 4a-c with $n_\parallel$ = 1.65 and $n_\perp$ = 1.50 are plotted in Fig. 5. The unwound helix is thus biaxial with exception of the case θ = 45°, where the anisotropy changes its sign.

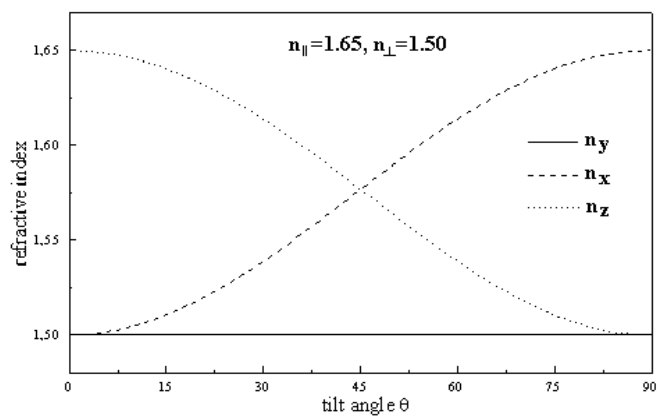

Figure 5. *Dependence of the refractive index components n_y, n_x (component 12 in Fig. 4), and n_z (component 11 in Fig. 4) on the molecular tilt angle θ.*

To describe all possible orientations of the molecules in the helical structure along its axis *z*, one has to consider the azimuth angle φ, which describes the rotation of the molecules around the *z*-axis. For a particular value of *z*, i. e. a particular value of φ, the local dielectric susceptibility tensor can be calculated using the corresponding geometric transformation of the tensor given in equation 3. Thus one gets:

$$\varepsilon_{xx}^{loc} = \varepsilon_\perp(\cos^2\theta\cos^2\varphi + \sin^2\varphi) + \varepsilon_\parallel \sin^2\theta\cos^2\varphi \tag{5a}$$

$$\varepsilon_{xy}^{loc} = \varepsilon_{yx}^{loc} = (\varepsilon_\perp - \varepsilon_\parallel)\sin^2\theta\sin\varphi\cos\varphi \tag{5b}$$

$$\varepsilon_{yy}^{loc} = \varepsilon_\perp(\cos^2\theta\sin^2\varphi + \cos^2\varphi) + \varepsilon_\parallel \sin^2\theta\sin^2\varphi \tag{5c}$$

$$\varepsilon_{zz}^{loc} = \varepsilon_{\perp} \sin^2\theta + \varepsilon_{\parallel} \cos^2\theta \tag{5d}$$

All other, not mentioned components are zero. The average values of the non-deformed helical structure can be calculated using the integration of equations 5a-d with respect to φ over a full turn 2π. Since the integrals of the non-diagonal elements (equation 5b) become zero, the refractive indices of the helical structure are calculated from the diagonal elements to:

$$< n_x > = < n_y > = \sqrt{[n_{\perp}^2 (1+\cos^2\theta) + n_{\parallel}^2 \sin^2\theta]/2} \tag{6a}$$

$$< n_z > = \sqrt{n_{\perp}^2 \sin^2\theta + n_{\parallel}^2 \cos^2\theta} \tag{6b}$$

These equations are also valid for the well known helical smectic C structure (Fig. 1). In Fig. 6 the effective refractive indices $<n_z>$ and $<n_x>$, calculated according to equations 6a, b are plotted for examples where the refractive indices of the sub-units 2 and 3 are equal to $n_{\parallel}$ = 1.65 and $n_{\perp}$ = 1.50, as well as $n_{\parallel}$ = 1.70 and $n_{\perp}$ = 1.45. It is seen that the anisotropy of the effective refractive index ellipsoid in dependence on tilt angle θ passes through zero (at θ = 54.7°) and changes its sign at further increase of θ.

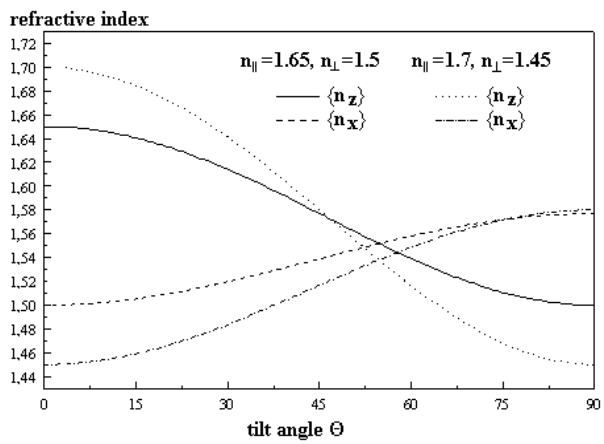

Figure 6. *Dependence of the components $<n_z>$ and $<n_x>$ of the averaged refractive index ellipsoid in ferroelectric liquid crystal with non-deformed helix on the molecular tilt angle θ.*

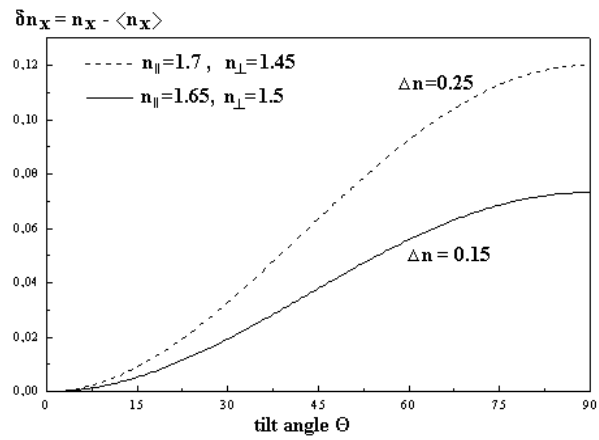

Figure 7. *Upper limit for the refractive index modulation, calculated as the difference between the refractive indices of to the totally untwisted and the non-deformed helix state*

The upper limit for the modulation of the refractive index is given by the difference of the indices of the totally unwound state n_x and of the undisturbed helix $<n_x>$. Because the index n_z remains constant (cf. equations 4c and 6b) and n_y is along the propagation direction of the light wave, only the change of the refractive index n_x will modulate the phase of a light wave polarized along the *x*-axis under the influence of an untwisting voltage. In Fig. 7 the calculated upper limit δ*n* of the index modulation is plotted versus the value of the tilt angle θ for two cases of the refractive indices of the sub-units 2 and 3, namely $n_{\parallel}$ = 1.65 and $n_{\perp}$ = 1.50 as well as $n_{\parallel}$ = 1.70 and $n_{\perp}$ = 1.45. In Table 1 some numerical data are presented.

It is worth noting, that the limit case of tilt angle θ = 90° optically corresponds to a nematic liquid crystal with negative refractive index anisotropy, as described by Thurmes et al. [22]. Provided that the described material MDW 1069 would have a smectic phase with a helical structure, the estimated change of the refractive index under an untwisting electric voltage could be about 0.05. Thus, a phase modulation of π could be obtained at a cell thickness of 11 - 12 µm.

	δn_x	
tilt angle θ, /°	($n_{\parallel}$ = 1.65 , $n_{\perp}$ = 1.50)	($n_{\parallel}$ = 1.70 and $n_{\perp}$ = 1.45)
20	0.0091	0.015
25	0.013	0.023
30	0.019	0.032
35	0.025	0.042
40	0.031	0.053
42	0.034	0.057
45	0.037	0.063

Table 1: *The upper limit δn_x for the change of the average refractive index $\delta n_x = n_x - \langle n_x \rangle$ under application of an electric field E, exceeding the threshold value E_c of untwisting, i. e. $E > E_c$.*

3. Estimation of the gray scale behavior of the refractive index n_x under influence of an electric field

For the calculation of average values of the refractive indices of the deformed helix structures from equations 5a-d, the non-uniform variation of the angle φ with the coordinate *z* along the helical axis in dependence on the electric field *E* must be considered. According to theory [17] the angle φ along the helix axis can be described in the linear regime (i. e. for electric field strengths considerably lower than the threshold value for unwinding) by

$$\varphi(z) = 2\pi z / p + \tilde{E} \cos(2\pi z / p) , \qquad (7)$$

where $\tilde{E}$ is the electric field *E* normalized to the critical field E_c for unwinding of the helix and *p* is the helical pitch. The average refractive indices for the deformed helix can thus be obtained by introducing expression 7 into equations 5a-d and performing numerical integrations with respect to *z* over a full helical pitch. Because of the given symmetry, the non-diagonal elements (cf. equation 5b) are zero even in this case and the orientation of the optical axes of the of the helical structure from banana shaped molecules keep unchanged from the field-free non-deformed state over the deformed state until (and including) the total unwound state. Thus only phase modulation without changing the state of polarization occurs under the influence of an electric field. In Figures 8 and 9 some results of numerical calculations are presented. In Fig. 8 the change of the refractive index n_x under the influence of an electric field E_y applied along the *y* axis of the helical structure is plotted (tilt angle θ = 40°). Two sets of molecular refractive indices 2' and 3' of the sub-units 2 and 3 are used: $n_{\parallel}$ = 1.65, $n_{\perp}$ = 1.50 and $n_{\parallel}$ = 1.70, $n_{\perp}$ = 1.45. In Fig. 9 the dependence of the change of the refractive index n_x on the normalized electric field is plotted for different values of the tilt angle θ, where the very good gray scale in the variation of n_x versus voltage is seen.

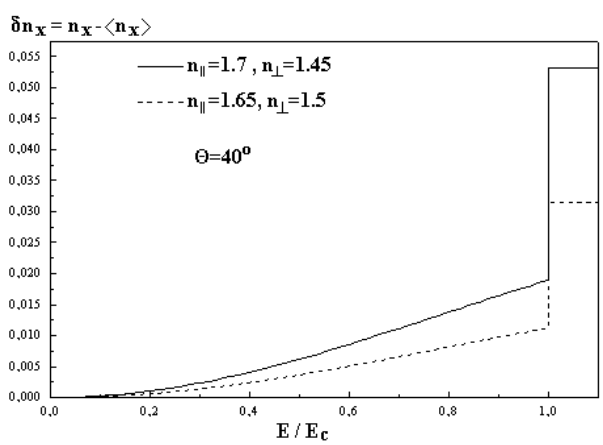

Figure 8. *The modulation δn_x of the refractive index component $\langle n_x \rangle$ under influence of an electric field for two different sets of molecular refractive indices.*

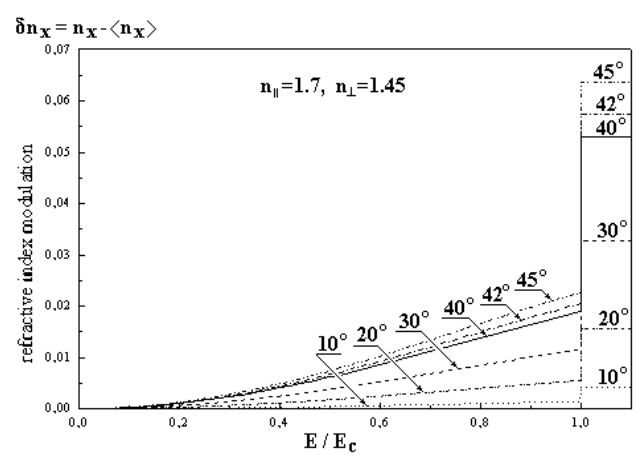

Figure 9. *The refractive index modulation δn_x under influence of the electric field at different tilt angles θ.*

The amplitude of the gray scale in $n_x(E)$ is almost proportional to the molecular tilt angle θ, and for θ = 40…45° the maximum change of n_x reaches 0.02. It means that a perfect gray scale for a phase shift 2π for a light wave with λ = 0.63 μm

will be at a cell thickness of the order of 30 μm. Using double passing of the light beam through the cell by means of a mirror behind the cell, the necessary thickness will be two time less, i. e. about 15 μm. In the regime of bistable switching between states with the phase difference 2π for an electric field E_y exceeding the threshold value E_c, the change of the refractive index n_x reaches 0.053…0.063. It means that the thickness of the FLC cell can be reduced to 10 μm in transmission mode and to 5 μm in reflection mode.

4. Possible chemical realization of the proposed liquid crystal.

Central cores 2 and 3: These fragments of the proposed liquid crystal can be chosen from any known cyclic component, used so far for the synthesis of liquid crystals. Commonly used phenyl, phenyl-pyrimidine, pyridine, terphenyl, biphenyl, biphenyl-pyrimidin and any other aromatic and/or polycyclic fragments can be used to provide the optically anisotropic central cores 2 and 3, which are characterized by the parallel and perpendicular refractive index components $n_{\parallel}$ and $n_{\perp}$ (cf. Fig. 4).

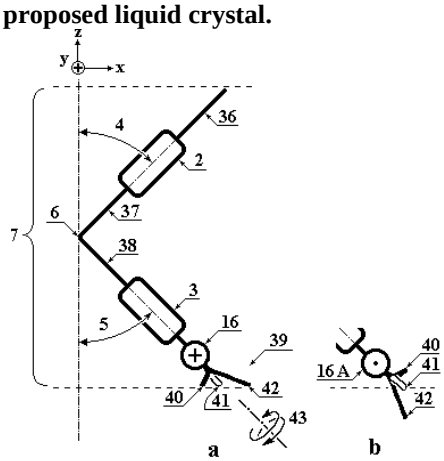

Figure 10. *The banana shaped dimer molecule, comprising two constituent central cores 2 and 3, the aliphatic chains 36, 37, 38, and a chiral fragment 39, formed by a tripod of molecular tails 40, 41, 42 of different length. A preferred orientation of the transversal dipole moment 16 occurs owing to the hindrance of the molecular librations 43 around the long axis of the constituent part of dimer, described by the fragments 38+3+16+39.*

Spontaneous polarization and molecular chirality: To realize a low voltage control of the azimuth 8, 9 of the tips 6 of the banana shaped molecules, the proposed molecules have a chiral fragment 39 (Fig. 10), which contains the dipole moment 16 apart from the central cores 2 and 3 responsible for the optical properties in the visible range of spectrum.

If such a molecule is embedded within a smectic layer 7, the dipole moment 16 will be directed in a certain direction *y* owing to the hindrance of the librations of the molecules along their long axis connecting the tip 6 and the chiral fragment 39. This hindrance has the same nature as it was described by R. B. Meyer [9] and is related with the monoclinic surrounding near the chiral fragment 39, composed from molecular tails 40, 41 and 42, which have different lengths and are usually formed by three different aliphatic and fluorinated fragments like

$$-C^*H(CH_3)C_nH_{2n+1} \quad \text{or} \quad -C^*H(CF_3)C_nH_{2n+1}\,,$$

where n = 2…8 (most preferable n = 3…6). The state as shown in Fig. 10a of such a molecule is more preferable than the state depicted in Fig. 10b. The dipole moments 16, attached to the chiral fragment 39 will have a transversal component along the normal to the inclination plane, i. e. along the *y* axis in Fig. 10. The dipole moments can be realized by different polar molecular groups like -CO-O-, -CO, $-CF_3$ and many others.

5. Obtaining a non-zero averaged spontaneous polarization within smectic layers using a polyphilic approach

If the dimer molecules are composed from two central cores 2 and 3, from aliphatic chains 36, 37, 38, and chiral fragment 39, with the dipole moment 16, the mutual cancellation of the spontaneous polarization induced by two molecules in a smectic layer can take place. It is connected with the presence of two equal possibilities to arrange the discussed molecules within the same smectic layer (cf. Fig. 11). In thermal equilibrium half of the molecules will have the orientation of the chiral fragments in the position 39 and the other half in position 39'. Dipole moments 16 and 16', respectively, will have opposite signs and are therefore compensated and no macroscopic spontaneous polarization will be observed. This compensation of polarization can be hindered by means of introducing a special fragment 44, based on a perfluorinated chain, into the banana shaped

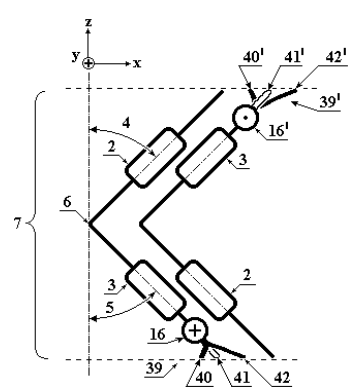

Figure 11. *Possible cancellation of the spontaneous polarization within a smectic layer due to symmetrical packing of two oppositely oriented molecules. Dipoles 16 and 16' have opposite directions.*

molecules. This perfluorinated fragment can have e. g. the following structure

$$-(CF_2)_n-,$$

where n = 4…16. Such fragments may be introduced into the dimers 1 instead of one aliphatic, e. g. hydrocarbon chain -$(CH_2)_n$- (for example instead of chain 36). They provide a strong polyphilic segregation of the molecular fragments within the smectic layers, as it was discovered by Tournilhac et al. [18, 19] for non-dimeric compounds with the structures as presented in Table 2. Here the data are given about tilt angles of the central core (optical tilt angle θ_{opt}) and about the tilt angles of the inclination of perfluorinated chain relative to the normal to the smectic layers (fluorinated tail tilt angle θ_F):

Table 2: *Examples of smectic C liquid crystals with fluorinated chains [18, 19].*

Tilt angle / **Material**	**Optical tilt angle θ_{opt}**	**Fluorinated tilt angle θ_F**
$F(CF_2)_8(CH_2)_{11}$-O-**Φ**-**Φ**-CN	48	28
$F(CF_2)_8(CH_2)_{11}$-O-**Φ**-$_N$**Φ**-CN	49	30
$F(CF_2)_8(CH_2)_{11}$-O-**Φ**-**Φ**-CO-O-CH_2CF_3	51	33
$F(CF_2)_8(CH_2)_{11}$-O-CO- **Φ**-**Φ**-O-CH_2CF_3 [19]	n.a.	n.a

Here the abbreviation **Φ** designates the phenyl ring  and $_N$**Φ** designates the pyridine ring 

According to X-ray data [19] the fluorinated chains form a sub-layer within a smectic layer. Namely this property of the fluorinated chains will prevent the compensation of dipole moments (cf. Fig. 12). The fluorinated chains 44, 44', 44", etc. form the sub-layer 44-1, preventing the flip-flop orientation of the molecules within one smectic layer 7. As a consequence the chiral fragments 39 will be collected in another sub-layer 39-1 within the same smectic layer 7. The symmetry of this sub-layer allows for the summarization of transversal dipole moments 16 near the chiral fragments 39 in the same direction *y* and thus for a macroscopic polarization.

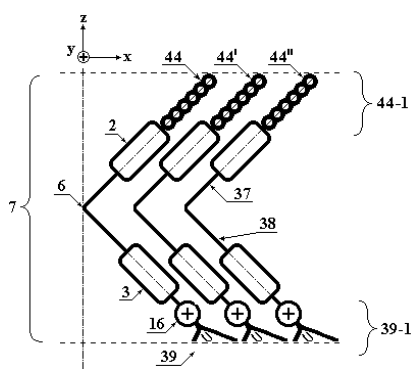

Figure 12. *The proposed structure of the polyphilic chiral banana shaped molecules, which form smectic layers with a spontaneous polarization. The tail 44 is formed for instance with the perfluorinated chain (-CF_2-)$_n$, which replaces the aliphatic hydrocarbon chain 36 of the molecule, shown in Fig. 11. Such tails form a sub-layer 44-1. This prevents the cancellation of the spontaneous polarization in the smectic layer 7. Dipole moments 16 of all molecules in smectic layer are directed in the same direction along the y-axis.*

An additional advantage of the fluorinated chains is connected with the (in comparison to analogous smectic liquid crystals with a hydrocarbon chain instead of the perfluorinated chain) higher optical tilt angle θ_{opt} (see Fig. 13) of the order 45° or more (see Table 1). The fluorinated tilt angle θ_F is much smaller than θ_{opt}, that is related with the larger area (27 Å^2) of the cross-section of this chain in comparison with the cross-section of the hydrocarbon chain (22 Å^2). Another advantage of the perfluorinated chain is the appreciable decrease of the rotational viscosity of the ferroelectric liquid crystal, and a very short response time less than 15 microseconds can be obtained [20].

In general, the perfluorinated fragment 44 should be in an asymmetric position relative to the tip 6 of the dimer. This can be realized in different ways: It may be introduced instead of the hydrocarbon chain 36 (as shown in Fig. 12), it can be added to this hydrocarbon chain 36 as end chain or tail (as shown in Fig. 13), or close to the central core 2. A position outside of the central cores is more preferable in comparison to the positions inside due to the higher

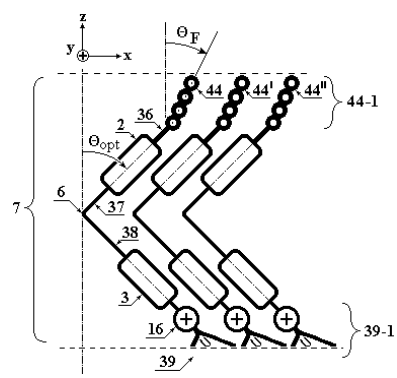

Figure 13. *The polyphilic molecules with the perfluorinated chain 44 connected to the aliphatic hydrcarbon tail 36 outside of the central core 2.*

polyphilic asymmetry of the dimers and hence a higher degree of segregation of perfluorinated fragments 44, 44', 44", etc. The chiral fragment 39 and the perfluorinated fragment 44 may be in the same or in different sub-units (2 or 3) of the dimer molecule.

Due to the chirality of the molecules the directions of tips 6 will form a helical structure in the electric field free state (Fig. 2, left part) with a uniform change of the azimuth angles 8, 9, etc. from layer to layer. An electric field E_y applied along the smectic layers will reorient the dipole moments 16 in the direction y and induce a corresponding reorientation of tips 6. For values of $E_y > E_c$ the helix will be totally unwound with the extreme state shown in the right part of Fig. 2.

6. Two chiral fragments in the banana shaped polyphilic dimers

The value of the spontaneous polarization related with the presence of the chiral fragment 39 and the transversal dipole moment 16 as well as the value of the pitch of helix can be strongly modified by means of introduction of a second chiral fragment 46 into the dimer molecules (cf. Fig. 14). In general this fragment should have a different shape and/or different value of the transversal dipole moment 45. The chiral fragment 46 can be realized using molecular fragments 47, 48 and 49, which are different from the constituent parts 40, 41, and 42, of the first chiral fragment 39 in the opposite sub-unit of the dimer. In the best case the dipolar moments 16 and 45 in both sub-units will have the same direction, as it is shown in Fig. 14. Otherwise, in case of opposite directions, the sum dipole moment of the sub-layers, and hence the value of the spontaneous polarization, will be determined by the difference between the values 45 and 16. In the worst case of equal values 45 and 16 the spontaneous polarization will be cancelled out.

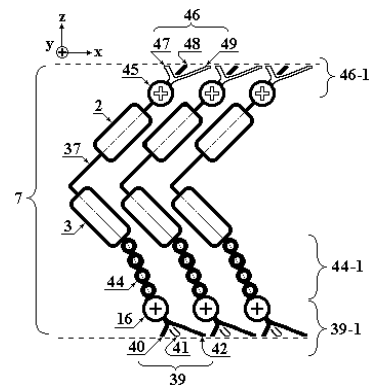

Figure 14. *The polyphilic dimer molecules having two chiral fragments 39 and 46 , and two transverse dipole moments 16 and 45. The perfluorinated chain 44 is introduced between central cores 3 and chiral fragment 39.*

7. Ferroelectric and antiferroelectric helical smectic liquid crystals composed from banana shape dimer molecules

The smectic layers 7 (Fig. 2), with the described banana shaped molecules 1 may form a ferroelectric packing of the neighbor layers as shown in Fig. 3a, if the sum dipole moments of the neighbor layers have the same directions in layers 7, 7-1 and so on. The neighbor smectic layers 7 and 7A may also form a antiferroelectric packing as shown in Fig. 3b, if the sum dipole moments of the neighbor layers have opposite directions. Mutual orientations of the tips 6 and 6A and sum dipole moments in the neighbor layers can have different combinations. E. g. the structure may be antiferroelectric, but tips 6 and 6A can be directed in the same direction (Fig. 15). Analogous options may be considered in case of molecules containing two chiral fragments as described in Fig. 14. E. g. in this case a antiferroelectric packing with opposite directions of tips in neighbor smectic layers is possible (Fig. 16). The optical properties of all ferroelectric as well as of all antiferroelectric structures are equal if the pitch of helix is smaller than the wavelength. They are characterized by an refractive index ellipsoid which doesn't change its initial orientation along the helix or along the normal to smectic layers z. Under influence of an electric field applied along the smectic layers (along the axis y) the refractive index component $\langle n_x \rangle$ along the x axis is increased and phase-only modulation takes place for the light polarization plane along x axis.

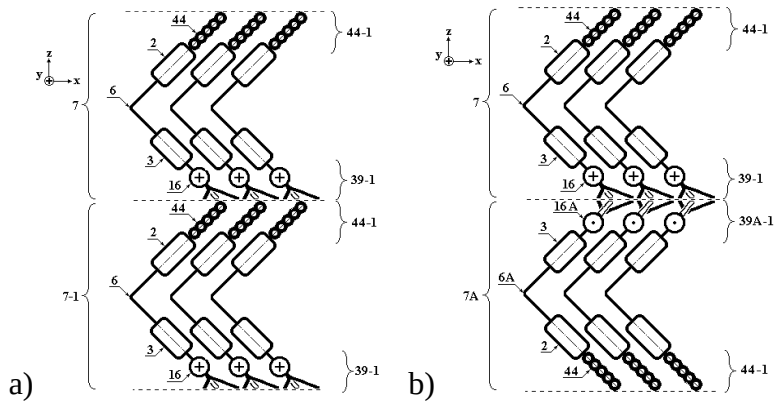

Figure 15. *Ferroelectric (a) and antiferroelectric (b) packing of the neighbor layers 7 and 7-1 with the summarization and cancellation of the dipole moments 16 of adjacent layers, respectively. The tips 6 of adjacent layers are directed in the same direction in both structures.*

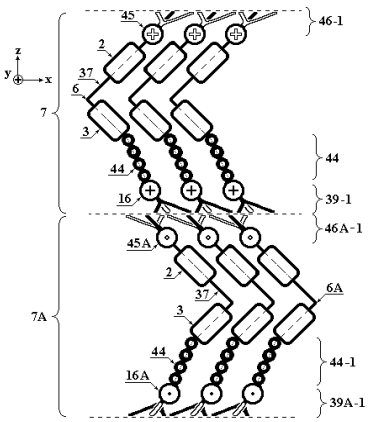

Figure 16. *Antiferroelectric packing of the neighbor layers 7 and 7A for dimer banana shaped molecules as shown in Fig. 14. The sum dipole moments as well as the tips 6 and 6A of neighbor layers have opposite directions*

4. USE OF THE PROPOSED LIQUID CRYSTALLINE MATERIAL FOR THE DESIGN OF PHASE MODULATORS

The described liquid crystals might be used for the design of different kind of phase modulators. The material should be introduced between electrodes, for instance between transparent ITO (indium tin oxide) electrodes. The smectic layers should be perpendicular to the electrode surfaces (Fig. 17). The polarization plane of the incident light should coincide with the smectic layers (*x*-axis).

The device may contain a multi-pixel electrode structure or photoconductive layer can be deposited above one ITO electrode for fabrication of an optically addressed spatial light phase modulator (OASLM). The OASLM may contain a mirror in contact with one surface of the proposed liquid crystal. In this case double passing of the light through the liquid crystal layer allows to reduce the thickness of the liquid crystal layer by a factor of 2 to obtain the same amplitude of phase modulation. The reflective type OASLM may contain a light absorbing layer to improve the decoupling between write light beam and read-out light beam, hence a light valve with high light amplification can be designed also (Fig. 18).

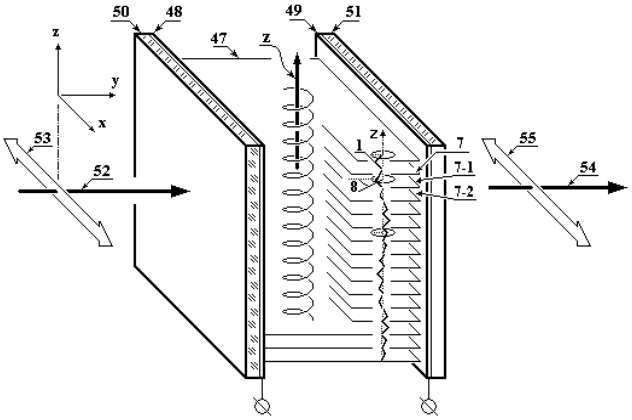

Figure 17. *Phase modulator based on the described liquid crystal. For the light polarization plane 53 of the light beam 52 along the axis x only a change of the refractive index takes place. The transmitted light beam 54 conserves the orientation of the polarization plane 55 along the x axis.*

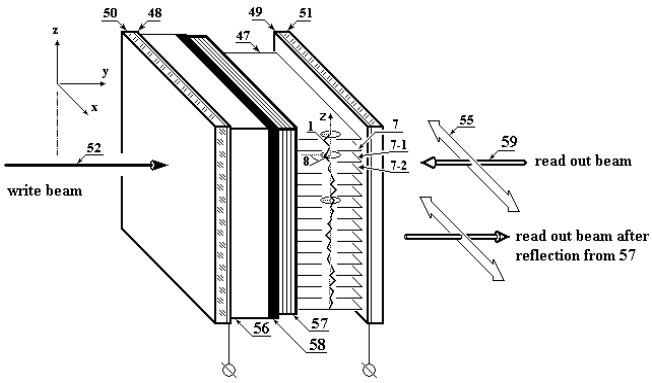

Figure 18. *Optically addressed spatial light phase modulator of the reflective type. The light absorbing layer 58 is introduced between the photoconducting layer 56 and the mirror 57.*

5. REFERENCES

1. R. K. Tyson "Principles of Adaptive Optics" (Academic, New York, 1991).
2. R. Q. Fugate "Laser beacon adaptive optics", *Opt. Photon. News*, June 1994, p. 14.
3. M. A. Vorontsov, G. W. Carhart, D. V. Pruidze, J. C. Ricklin, and D. G. Voelz "Image quality criteria for an adaptive imaging system based on statistical analysis of the speckle field", *J. Opt. Soc. Am. A*, **13(**7), 1456 (1996).
4. J. C. Ricklin, "Optical technique for simulating severe phase distortion effects in imaging system performance", *Opt. Photon. News*, Dec. 1995, pp. 15-16.
5. T. Sonehara and J. Amako, "Phase modulated liquid crystal spatial light modulator with VGA resolution", in: Technical Digest of OSA Topical Spring Meeting "Spatial Light Modulators", March 17-19, 1997, Hyatt Regency Lake Tahoe, Incline Village, Nevada USA, p.120, STuE7-1.
6. N. Mukohzaka, N. Yoshida, H. Toyoda, Yuji Kobayashi, and T. Hara, "Diffraction efficiency analysis of a parallel-aligned nematic-liquid-crystal spatial light modulator", *Applied Optics*, **33**(14), 2804 (1994).
7. L. M. Blinov and V. G. Chigrinov, "Electrooptic effects in Liquid Crystal Materials", (Springer, New York, 1993).
8. 128x128 Analog Liquid Crystal Spatial Light Modulator, Specification of Boulder Nonlinear Systems, Inc., Boulder, CO U.S.A.
9. R. B. Meyer, L. Liebert, L. Strzelecky, and P. Keller, "Ferroelectric liquid crystals", *J. de Physique-Lett.* (Paris), **L-69,** 36, (1975).
10. N. A. Clark, and S. T. Lagerwall, "Submicrosecond bistable electro-optic switching in liquid crystals", *Appl. Phys. Lett.*, **36**, 899 (1980)
11. S. T. Lagerwall, N. A. Clark, J. Dijon, and J. F. Clerc, "Ferroelectric liquid crystals: the development of devices", *Ferroelectrics*, **94**, 3 (1989).
12. L. A. Beresnev, V. G. Chigrinov, D. I. Dergachev, M. V. Loseva, N. I. Chernova, E. P. Pozhidaev, B. I. Ostrovskii, A. Z. Rabinovich, A. V. Ivaschenko, V. V. Titov and M. Schadt, Swiss Patent, 3722/87, Ref. RAN 4701/127-002, priority 21 Sept. 1987, "Ferroelektrische Flüssigkristallanzeige".
13. L. A. Beresnev, V. G. Chigrinov, D. I. Dergachev, E. P. Pozhidayev, J. Fuenfschilling, and M. Schadt, "Deformed helix ferroelectric liquid crystal display: A new electrooptical mode in ferroelectric chiral smectic C liquid crystals", *Liquid Crystals*, **5**, 1171 (1989).
14. L. A. Beresnev, L. M. Blinov and D. I. Dergachev, "Electrooptical response of a thin layer of a ferroelectric liquid crystal with a small pitch and high spontaneous polarization", *Ferroelectrics*, **85**, 173 (1988).
15. W. K. Choi, A. B. Davey and W. A. Crossland, "Use of deformed helix ferroelectric liquid crystals in Fabri Perot etalons", *Ferroelectrics*, **181**, 11 (1996).
16. J. Eschler, S. Dickmann and D. A. Mlynski, "Fast adaptive lens based on deformed helical ferroelectric ciquid crystal", *Ferroelectrics*, **181**, 21 (1996).
17. S. A. Pikin, "Structural transformation in liquid crystals", (Gordon & Breach, New York, 1991).
18. F. Tournilhac and J. Simon, "Structural properties of polyphilic mesogens. Toward longitudinal ferroelectricity", *Ferroelectrics*, **114**, 283 (1991).
19. F. G. Tournilhac, L. Bosio, J. Simon, L. M. Blinov, and S. V. Jablonsky, "Synthesis of polyphilic compounds. Evidence for ferroelectricity in a non-chiral mesophase", *Liquid Crystals*, **14**, 405 (1993).
20. H. Liu and H. Nohira, "Synthesis of semi-perfluorinated FLCs and the effect of fluorination extent on mesomorphic properties", *Mol. Cryst. Liq. Cryst.*, **302**, 257 (1997).
21. G. Pelzl, S. Diele, S. Grande, A. Jakli, Ch. Lischka, H. Kresse, H. Schmalfuss, I. Wirth, W. Weissflog, "Structural and electro-optical investigations of the smectic phase of chlorine-substituted banana-shaped compounds", *Liquid Crystals*, **26**, 401-413 (1999).
22. W. N. Thurmes, M. D. Wand, R. T. Vohra, C. M. Crandall, J. Xue, and D. M Walba, "Negative birefringence ferroelectric liquid crystals", *Liquid Crystals*, **25**, 149 (1998).